scientific reports

Check for updates

OPEN

Contracting eastern African C_4 grasslands during the extinction of *Paranthropus boisei*

Rhonda L. Quinn[1,2]✉ & Christopher J. Lepre[2]

The extinction of the *Paranthropus boisei* estimated to just before 1 Ma occurred when C_4 grasslands dominated landscapes of the Eastern African Rift System (EARS). *P. boisei* has been characterized as an herbivorous C_4 specialist, and paradoxically, its demise coincided with habitats favorable to its dietary ecology. Here we report new pedogenic carbonate stable carbon ($\delta^{13}C_{PC}$) and oxygen ($\delta^{18}O_{PC}$) values (nodules = 53, analyses = 95) from an under-sampled interval (1.4–0.7 Ma) in the Turkana Basin (Kenya), one of the most fossiliferous locales of *P. boisei*. We combined our new results with published $\delta^{13}C_{PC}$ values from the EARS dated to 3–0 Ma, conducted time-series analysis of woody cover (f_{WC}), and compared the EARS f_{WC} trends to regional and global paleo-environmental and -climatic datasets. Our results demonstrate that the long-term rise of C_4 grasslands was punctuated by a transient but significant increase in C_3 vegetation and warmer temperatures, coincident with the Mid-Pleistocene Transition (1.3–0.7 Ma) and implicating a short-term rise in pCO_2. The contraction of C_4 grasslands escalated dietary competition amongst the abundant C_4-feeders, likely influencing *P. boisei*'s demise.

Since Leakey and colleagues[1] (pg. 9) suggested *Paranthropus boisei* was the "victim" of *Homo habilis* at Olduvai (Oldupai) Gorge (Tanzania), our ancestors have been implicated in the demise of their sister taxon. Tool-assisted foraging behaviors were traditionally thought to have propelled genus *Homo* into a broad omnivorous dietary niche, providing an evolutionary edge relative to *Paranthropus*' dentognathic procurement strategies across Africa's savanna habitats[2] and resulting in competitive exclusion[3]. More recent archaeological evidence suggests that both *Homo* and *Paranthropus* were plausible inheritors of tool-making behaviors[4,5], and stable carbon isotopic ($\delta^{13}C_{enamel}$) and microwear analyses of fossil specimens have revealed a dynamic and complex evolutionary history of Pleistocene African hominin and non-hominin primate diets (Fig. 1)[6–13]. Eastern African hominins and *Theropithecus*, the large-bodied baboon, underwent a dietary transition incorporating more C_4 foods in the early Pleistocene[6,8,9,12], which have been attributed to behavioral changes in response to complex competitive landscapes[12]. Distinct from other Pleistocene hominins, *P. boisei*, the last eastern African paranthropine species, yielded $\delta^{13}C_{enamel}$ and $\delta^{44/42}Ca_{enamel}$ values indicating a herbivorous[13] and primarily C_4 diet[6] from ~ 2.3 Ma until its last appearance from the fossil record at ~ 1.3 Ma[14]. Unexpectedly, isotopic evidence for this shift into a C_4-plant feeding niche was not mirrored by changes in microwear patterns or dentognathic morphology[7,10,15]. *P. boisei's* diet had comparable mechanical properties to those of C_3-C_4-mixed feeding hominins such as *Australopithecus afarensis*[7]. *P. boisei's* use of fallback foods, rather than its dietary staples of C_4 plants, may have been the main influence for its distinctive "nut-cracking" form[7,10].

Wood and Patterson (2020)[16] suggested that *P. boisei's* 1-myr morphological and dietary stasis signifies that its occupied niche and associated adaptations were "remarkably durable." Although eastern African hominins may have begun their evolutionary trajectories as C_3-C_4-mixed-feeding opportunists during the early Pleistocene[11], *P. boisei* evolved to be a C_4 plant specialist[13] sharing more dietary similarities to *T. oswaldi* than with members of genus *Homo*, who remained C_3-C_4-mixed feeding omnivores (Fig. 1A–C). Thus evidence for dietary niche separation and shared stone tool making abilities cast doubt on competitive exclusion by *Homo* as a primary cause of *P. boisei's* demise.

A prevailing explanation for *P. boisei's* extinction is the opposite cause of *Homo*'s success, that is, its dietary and behavioral *inflexibility* amidst environmental perturbations[17]. *P. boisei's* extinction, estimated between 1.3 Ma[14] and just prior to 1 Ma[18], occurs during one of *Homo's* significant increases in brain size and its second wave of dispersal out of Africa and into Eurasia[19,20]. These evolutionary events in the hominin lineage are coincident with the Mid-Pleistocene Transition (MPT; 1.3–0.7 Ma)[21], when the Earth's glacial and interglacial climatic

[1]Department of Sociology, Anthropology, Social Work and Criminal Justice, Seton Hall University, 400 South Orange Ave, South Orange, NJ 07079, USA. [2]Department of Earth and Planetary Sciences, Rutgers University, 610 Taylor Road, Piscataway, NJ 08854, USA. ✉email: rhonda.quinn@shu.edu

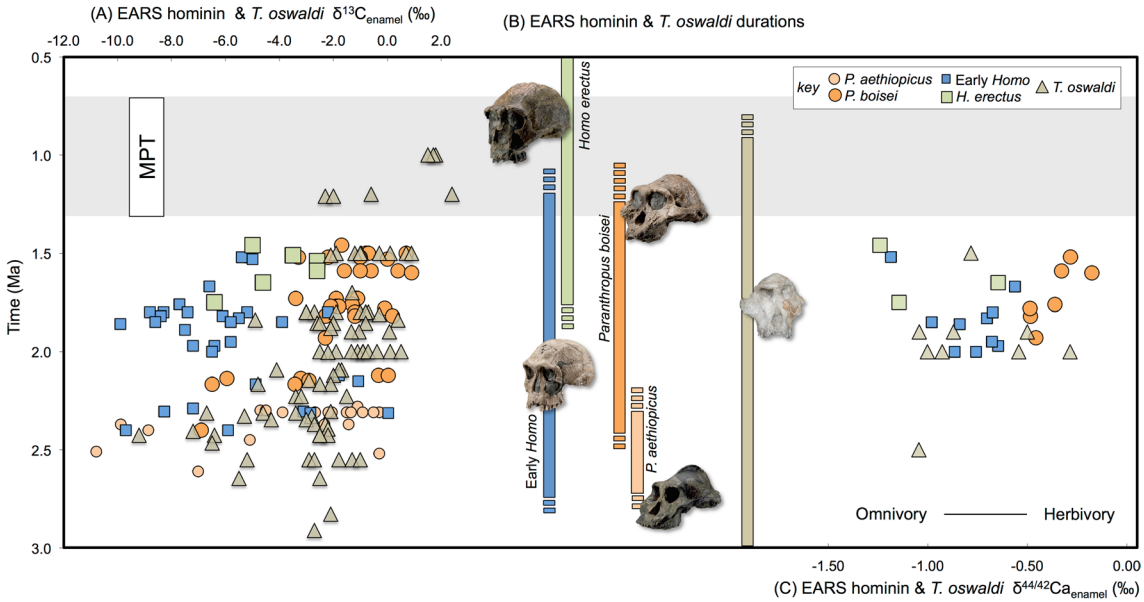

Figure 1. (**A**) $\delta^{13}C_{enamel}$ values of EARS hominins and *Theropithecus oswaldi* (**B**) duration generalized taxonomic groupings of EARS fossil hominins, (**C**) $\delta^{44/42}Ca_{enamel}$ values of EARS hominin and *T. oswaldi*. See Supplementary Data and Supplementary Information for specimen information, isotopic values, fossil image credits, and references. Shaded area denotes MPT interval (1.3–0.7 Ma).

intervals transitioned from an obliquity-paced (41-kyr) cyclicity to an asymmetrical ~ 100 kyr eccentricity pattern of repeated saw-toothed glacial growth and rapid deglaciation[22]. Global climatic and environmental changes are commonly evoked as major forces of eastern African hominin evolution[23]. Dietary and technological adaptations in the Plio-Pleistocene have been contextualized in open[24] and variable[25] landscapes, shaped by the presence of C_4 plant communities[24]. During the MPT interval, current environmental proxy records from the East African Rift System (EARS) show evidence for low percentages of woody cover[24] and high abundances of C_4-feeders[26–29]. This scenario begs the question: why would *P. boisei*, this "durable" herbivorous C_4-feeding hominin, disappear during the dominance of C_4 grasslands?

Here we report pedogenic carbonate stable carbon ($\delta^{13}C_{PC}$) and oxygen ($\delta^{18}O_{PC}$) isotopic values (nodules = 53, paired analyses = 95) in the Turkana Basin, northern Kenya, eastern Africa (Fig. 2A–C), from 1.4 to 0.7 Ma, an under-sampled interval for pedogenic carbonates in an otherwise well-studied region of human evolutionary environments (see "Methods", "Supplementary Information"). The Turkana region is the most fossiliferous of the known *P. boisei* sites[18], and Turkana specimens constitute the majority of isotopically analyzed *P. boisei* enamel samples to date[6,8,12,13]. We combine our new $\delta^{13}C_{PC}$ data to those from other EARS locations preserving the MPT interval, calculate fraction of woody canopy cover (f_{WC})[24], and compare the EARS f_{WC} record to other environmental, ecological and climatic proxy records from 3 to 0 Ma to examine the contexts of *P. boisei's* extinction.

Results

In contrast to characterizations of the Turkana Basin during the MPT as extremely grassy and dry[23,24,28,29], our new data (n = 53, 95 paired analyses) show excursions to lower $\delta^{13}C_{PC}$ and $\delta^{18}O_{PC}$ values, consistent with relatively woodier vegetation structures and more humid and/or warmer conditions (Supplementary Fig. S5). Exponentially smoothed f_{WC} and $\delta^{18}O_{PC}$ values from the Turkana Basin show temporally corresponding peaks of the excursions at 1 Ma (Supplementary Fig. S6). Exponential (Fig. 3A) and Loess (Fig. 3B) smoothing of the compiled EARS f_{WC} record from 3 to 0 Ma illustrate the long-term increase in C_4 vegetation punctuated by a short-term increase in C_3 vegetation beginning at the start of the MPT interval and peaking at 1 Ma. The interpreted pattern from the EARS f_{WC} record is substantiated with Bayesian change point analysis detecting two significant changes, which appear to mark the MPT interval (Fig. 3C).

African basins have idiosyncratic variables (e.g., elevation, topography, temperature, water deficits, tectonism) that influence the distribution of vegetation and local climatic conditions[23,30]. Individual EARS basins during the time of *P. boisei's* evolutionary history show local-scale heterogeneity in vegetation structures (Supplementary Fig. S7). Some EARS sites have low $\delta^{13}C_{PC}$ sampling resolutions or may be oversampled in specific time horizons. The Awash (Ethiopia) and Turkana (Kenya) basins have the highest $\delta^{13}C_{PC}$ sampling resolutions across the MPT interval (1.3–0.7 Ma)[21] with 27 and 53 samples, respectively, and both record significant reductions in C_4 vegetation (Supplementary Fig. S7). Olduvai (Oldupai) Gorge and Tugen Hills, yielding small sample sizes from the MPT interval, i.e., 12 and 3, respectively, show persistent grassy vegetation structures (Supplementary Fig. S7). Differences in vegetation structures between the northern and central EARS may be an artifact of low sampling density in the central EARS or true spatial differences within the EARS.

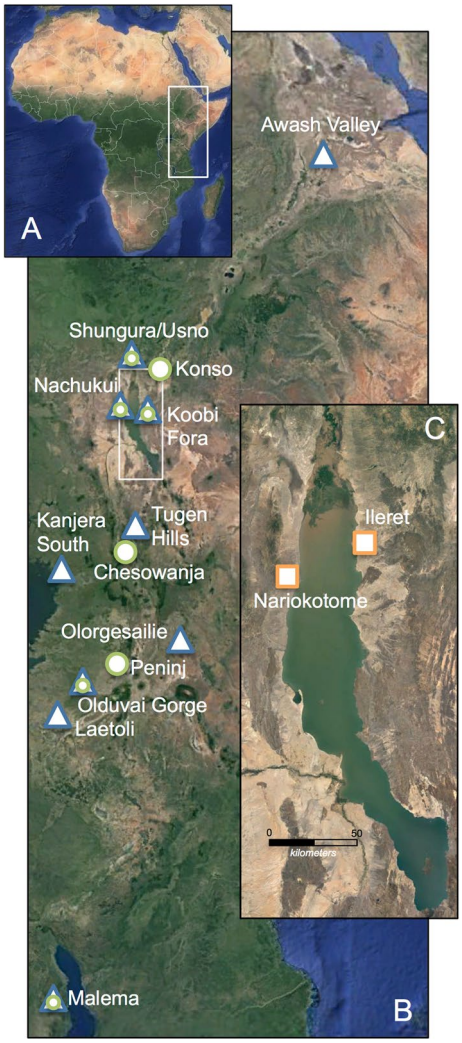

Figure 2. (**A**) Map of Africa with box outline showing (**B**) map of East African Rift System (EARS) with box outline showing (**C**) Turkana Basin (base map: Google Maps /TerraMetrics 2021). *P. boisei* fossil sites[18] are denoted with a circle. Sampling locations for EARS f_{WC} data that also preserved *P. boisei* specimens are marked with a circle embedded in a triangle. EARS f_{WC} data from sites that did not yield *P. boisei* fossils are denoted with a triangle. Squares in inset map mark the locations of new $\delta^{13}C_{PC}$ and $\delta^{18}O_{PC}$ data presented in this study.

Discussion

Causes of the EARS C_3 excursion. Vegetation structures are dependent on mean annual precipitation (MAP)[31], and increasing abundances of C_3 vegetation would be predicted with higher rainfall during the MPT. Several mechanisms are proposed to have altered water delivery to Plio-Pleistocene Africa, including eccentricity-modulated precession, glacial forcing of the Inter-Tropical Convergence Zone (ITCZ) position, and tropical sea-surface temperature fluctuations among others[33–38], yet regional proxy records yield dissimilar evidence for hydroclimate (Fig. 4A–E). Dust flux data from marine cores at sites 721/722 in the Arabian Sea indicate several intervals of increased aridity, including one circa 1 Ma (Fig. 4A)[35]. In contrast, deep lakes in the EARS are thought to have formed during periods of higher rainfall and forced by 405-kyr eccentricity (insolation) maxima (Fig. 4B)[36]. During the MPT, Lake Silbo was present in the Turkana Basin[39,40], possibly indicating higher rainfall.

Recent studies have suggested that hydroclimate may not be the primary cause of changes to African vegetation structures[38,41,42]. Plant wax δD values from ODP cores 235/241 in the Indian Ocean off of eastern Africa indicate no directional trend in calculated precipitation δD over the last 10 million years, and the MPT interval in those cores, specifically, does not appear to have experienced a significant shift in regional paleohydrology yielding intermediate values within the 3–0 Ma study interval (Fig. 4C)[38]. However, the sampling density (n = 3) of ODP 235/241 through the MPT is of particularly low resolution. If orbital climate forcing[36] was the primary influence of the EARS C_3 excursion, we would predict multiple C_3 excursions coinciding with insolation maxima, which is not the case (Fig. 4D). The Turkana Basin $\delta^{18}O_{PC}$ record, a proxy of rainfall source, rainfall amounts, and/or temperature, shows a long-term trend consistent with more arid and/or cooler conditions, followed by

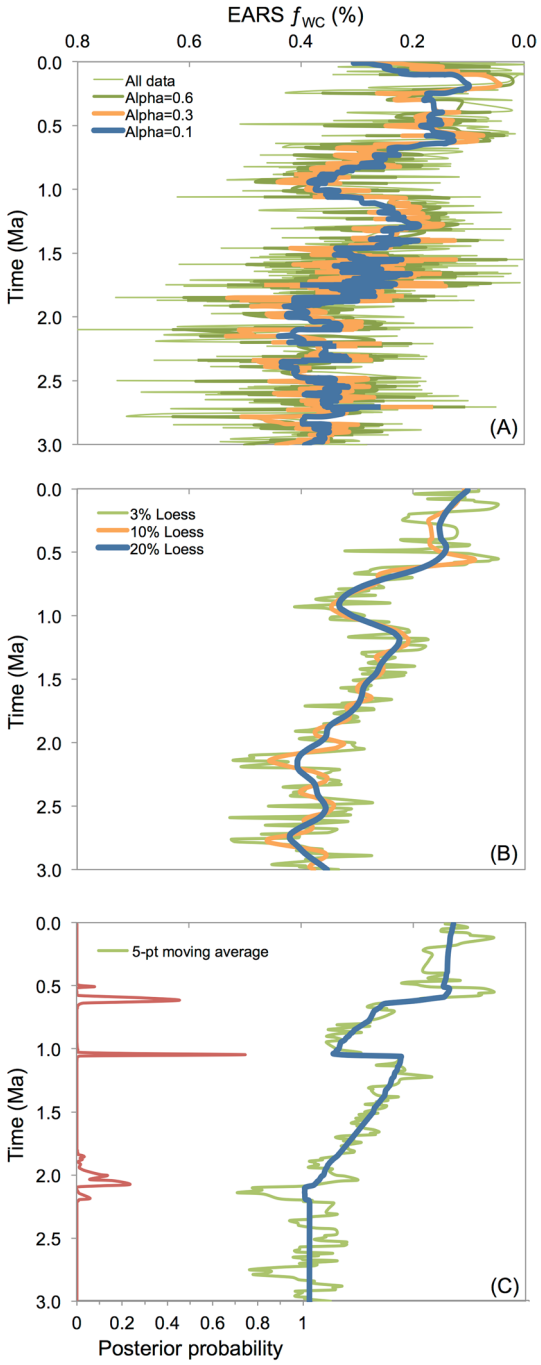

Figure 3. EARS f_{WC} data fitted with (**A**) simple exponential smoothed curves (α = 0.1, 0.3, 0.6), (**B**) loess regressions (3%, 10%, 20%) and (**C**) Bayesian change point algorithm of a 5-point moving average; posterior probabilities on secondary axis (red line). See Supplementary Data for site locations, $\delta^{13}C_{PC}$ values, and references. Shaded area denotes MPT interval (1.3–0.7 Ma).

a return to warmer and/or wetter conditions during the MPT (Fig. 4E). Additional rainfall proxy records from the EARS, able to distinguish rainfall amount from sources of rain[42,43], are warranted to further test for links between hydroclimate and vegetation structure.

Vegetation structures are impacted by herbivore communities[31]; thus major changes in animal community compositions may have influenced the EARS C_3 excursion (Fig. 5A–D). Significant declines in eastern African large-bodied carnivore speciosity from ~ 4–1 Ma (Fig. 5B)[44] and megaherbivore diversity from ~ 6 to 0 Ma (Fig. 5D)[41] correspond to the long-term EARS C_4 trend (Fig. 5A). C_3-browsing by fewer megaherbivores could have resulted in an increase in woody cover. However, after the C_3 excursion, the EARS f_{WC} record returns to previous percentages, maintaining the long-term C_4 trend, which is not predicted as megaherbivores continued to decline. A recent compilation of the number of EARS grazer species from ~ 7 to 0 Ma[45] parallels the spread of

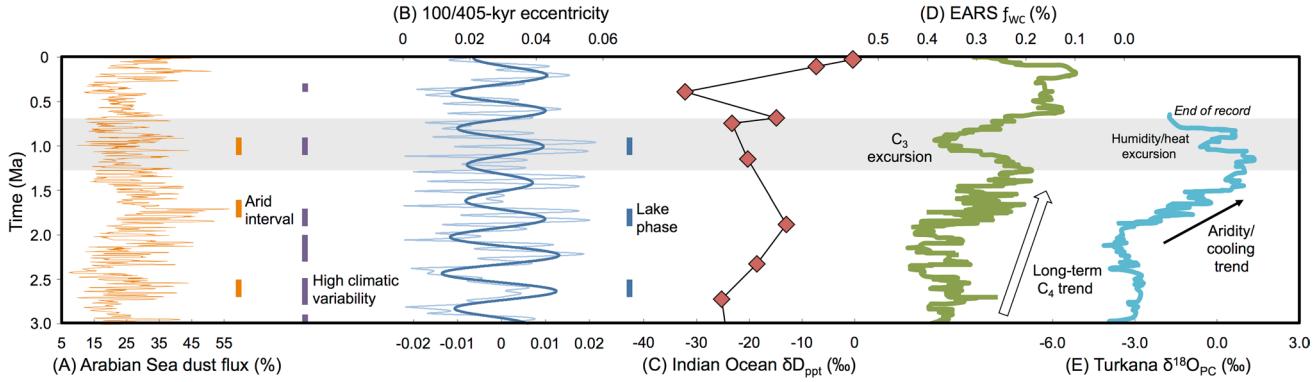

Figure 4. (**A**) Arabian Sea dust flux (%) from core sites 721/722 with proposed periods of increased aridity (orange bars)[35] and heightened environmental variability[25] (purple bars). (**B**) 100/405-kyr eccentricity record and proposed EARS lake phases[36] (blue bars). (**C**) plant wax δD_{ppt} values from Indian Ocean core sites 235/241[38], (**D**) EARS f_{WC} record (exponentially smoothed, $\alpha = 0.1$) (**E**) Turkana Basin $\delta^{18}O_{PC}$ values. See Supplementary Data and Supplementary Information for site locations, $\delta^{18}O_{PC}$ values, and references. Shaded area denotes MPT interval (1.3–0.7 Ma).

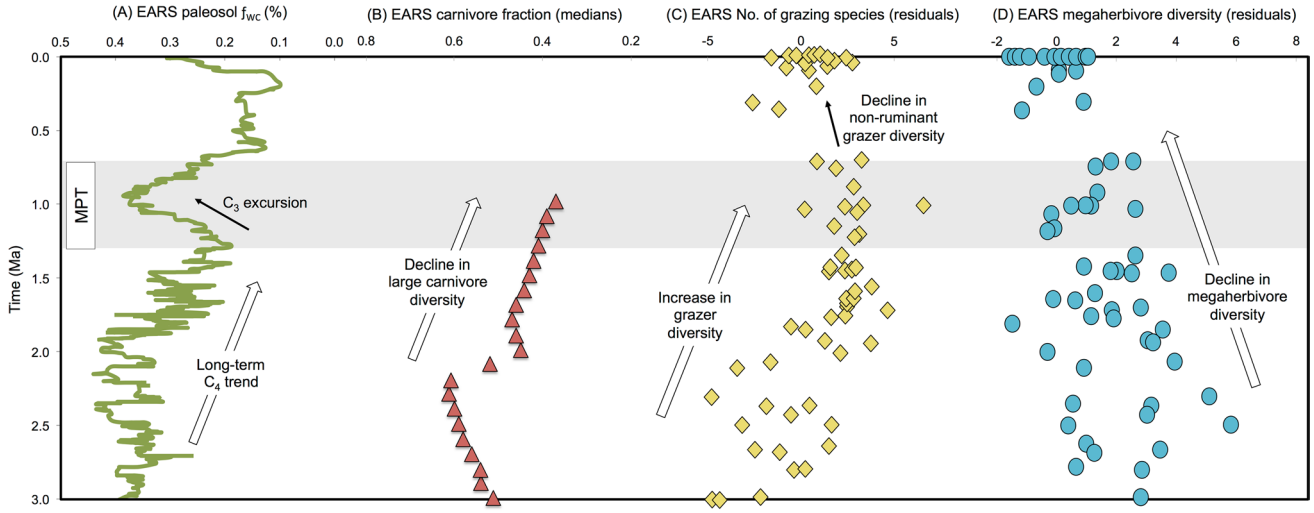

Figure 5. (**A**) EARS f_{WC} record (exponentially smoothed, $\alpha = 0.1$) compared to EARS fossil faunal abundance data: (**B**) carnivore fraction (medians);[44] (**C**) number of grazing species (residuals);[45] (**D**) megaherbivore diversity (residuals)[41]. Shaded area denotes MPT interval (1.3–0.7 Ma).

C_4 grasslands as previous shown[23,26,28]; however, there is a major decline in the number of EARS grazer species, specifically non-ruminant grazers, beginning at ~ 1 Ma and coincident with the peak of the EARS C_3 excursion (Fig. 5C). Faith and colleagues[45] proposed that non-ruminant grazers were outcompeted by ruminant grazers and mixed feeders due to habitat loss during aridity pulses beginning with the MPT. The Turkana Basin $\delta^{18}O_{PC}$ record is not consistent with increased aridity during the MPT, but the EARS f_{WC} record indicates that C_4 grasslands contracted significantly, which may have influenced the decline in non-ruminant grazers.

The long-term increase in eastern African C_4 grasslands and its impact on faunal communities has been associated to concurrently decreasing pCO_2[38,41]. Global climate and vegetation models[46,47] predict the cause-effect relationship between higher pCO_2 and destabilized C_4 vegetation[48]; moreover, woody thickening is proposed as a consequence of rising pCO_2[46,47]. Modeled and proxy pCO_2 records, showing discrepancies in estimations across the MPT (Fig. 6A–E), fuel various hypotheses about the role of pCO_2 in Earth's climatic reorganization[21,22,49–51]. The EARS f_{WC} record (Fig. 6G) is consistent with the Chinese Loess Plateau paleosol pCO_2 record[49] (Fig. 6E) and one of the pCO_2 models[51] (Fig. 6A) indicating relatively higher pCO_2 confined to the MPT interval. The clumped-isotope paleo-thermometer record, derived from paleosols in the Nachukui Formation at Turkana, shows higher temperatures during the MPT (Fig. 6F)[52], which are predicted with increasing pCO_2[53]. The Turkana Basin $\delta^{18}O_{PC}$ excursion circa 1 Ma is also consistent with higher temperatures (Fig. 4E).

We interpret that the EARS C_3 excursion was primarily forced by a transient increase in pCO_2, potentially accompanied by an increase in temperature. There is debate, however, about the primary drivers of African vegetation change[38,54], and vegetation proxy records from various African regions record dissimilar trends across the MPT. Plant wax $\delta^{13}C$ data from ODP core 1077 in the Lower Congo Basin indicated an increase in C_4 vegetation, which was interpreted as a response to an increased aridity circa 900 Ka[34]. Arabian Sea plant wax $\delta^{13}C$ data (core

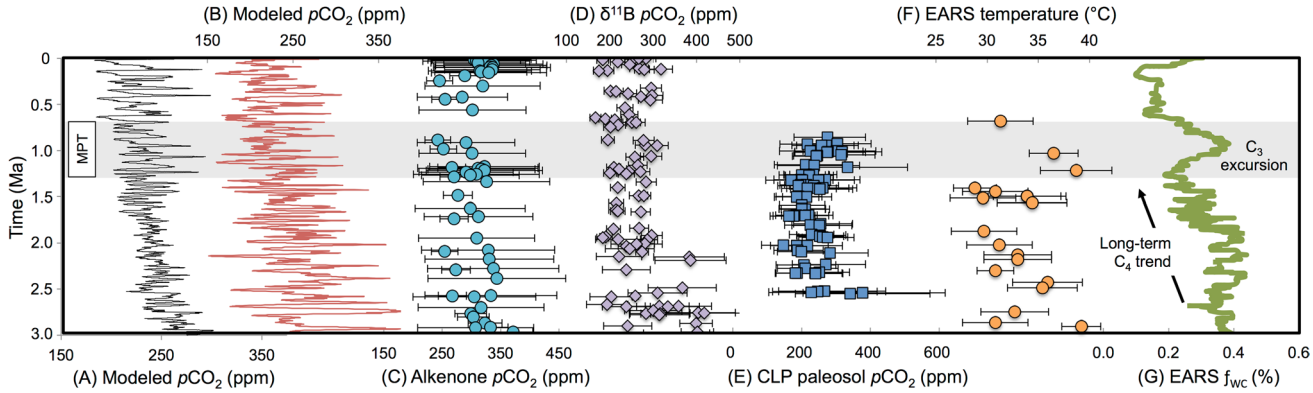

Figure 6. (**A**) Modeled global pCO_2;[51] (**B**) modeled global pCO_2;[50] estimated pCO_2 (ppm) derived from compiled (**C**) phytoplankton-alkenone records[23], (**D**) compiled $\delta^{11}B$ values[23], (**E**) Chinese Loess Plateau (CLP) paleosols[51], (**F**) paleotemperature estimates based on clumped isotope analysis of EARS pedogenic carbonates[52], (**G**) EARS f_{WC} record (exponentially smoothed, $\alpha = 0.1$). Shaded area denotes MPT interval (1.3–0.7 Ma).

sites 721/722) yielded evidence for a long-term increase in C_4 vegetation but no significant change during the MPT interval[38]. Lake Malawi plant wax $\delta^{13}C$ record, from the southern EARS (Malawi Rift), shows persistent C_3 vegetation throughout the Plio-Pleistocene and across the MPT interval[55]. Our analysis of individual basins demonstrates that the C_3 excursion occurred in the northern EARS and may not have been a significant event in the central EARS. However, we emphasize that sampling resolution of some of these records may not be sufficiently high to resolve vegetation changes within the MPT interval.

Finding discrepancies between the EARS f_{WC} record and other regional vegetation datasets supports interpretations that marine sediments to the north and west of Africa may not capture the complete range of paleoenvironmental conditions within the EARS[56,57]. In contrast to the limited spatial averaging of pedogenic carbonates (see Supplementary Information), marine core records of terrestrial vegetation represent integrated signals without specific provenance for large regions, for example, aeolian transport from southern Africa in the case of ODP core 1077[34]. Site- and region-specific controls on vegetation may differentially respond to changes in ice volume, sea surface temperatures, and pCO_2[38,57]. Moreover, model data and lake core studies demonstrate that rift basins respond differently to global environmental change such as during the Last Glacial Maximum[58,59]. Therefore, we suggest that a transient rise in global pCO_2 causing the EARS C_3 excursion does not necessitate synchronous declines in C_4 vegetation in other African regions.

A new behavioral and ecological scenario for the extinction of *P. boisei*. *P. boisei's* extinction occurred during a significant contraction of C_4 grasslands within the EARS, and specifically in one of its known habitats, the Turkana Basin. Admittedly, f_{WC} estimates do not fully characterize the diversity and complexities of African vegetation communities during the Pleistocene, but rather provide evidence for relative changes in the dominant (C_3 vs. C_4) vegetation structures. The decline in C_4 grasslands likely resulted in the loss of *P. boisei's* exploited C_4 plant foods (Fig. 7A), but the identities of those C_4 plant foods remain unknown. Microwear evidence suggest that foods items may not have involved hard components[7,10] but rather "novel mechanical challenges" entailing masticating C_4 grasses and sedges for long periods of time[12]. Faunal-based studies have emphasized that EARS environments during human evolution were "non-analogous" to modern faunal community structures[26,45,60]. In a common thread, paleovegetation communities also evolved through time, thus limiting the use of modern EARS environments and current vegetation proxy methods to identify specific elements of vegetation communities as well as particular plant species consumed by Pleistocene hominins. Moreover, dietary reconstructions of eastern African hominins and non-hominin primates with $\delta^{13}C_{enamel}$ and $\delta^{44/42}Ca_{enamel}$ data pose issues of isotopic equifinality[61] where many types of food combinations may result in comparable isotopic values.

P. boisei likely competed directly with the EARS grazing species for C_4 plant foods (Fig. 7B). We suggest that *P. boisei* and several other non-ruminant grazers were outcompeted by ruminant grazers for declining C_4 plant foods during the MPT interval. Of course, *P. boisei* was not an herbivorous ungulate but rather a large-bodied, bipedal, encephalized, and likely stone tool using hominin[15,18,62], thus its life history strategies, social organization, reproductive rates, activity times, caloric and nutritional requirements, home and day ranges, and cognitive abilities were likely more similar to other hominins and non-hominin primates than to most of the ungulates occupying the EARS C_4 biome. *T. oswaldi* was likely in direct competition with *P. boisei* for C_4 plant foods throughout the Pleistocene (Fig. 7C). $\delta^{44/42}Ca_{enamel}$ values, however, suggest that *T. oswaldi* engaged in omnivory throughout its evolutionary history, providing some dietary niche separation from the herbivorous *P. boisei* but also a competitive advantage, as C_4 plant foods contracted.

Although much evidence indicates dietary niche partitioning between *P. boisei* and members of *Homo*, some dietary competition may have occurred. Patterson and colleagues (2019)[63] suggested that in the Koobi Fora region of the Turkana Basin after 1.65 Ma, *Homo* sp. $\delta^{13}C_{enamel}$ values slightly converge with those of *P. boisei,* and *H. erectus* was by and large the C_4 interloper (Fig. 1). The post-1.65 Ma change in *Homo* sp. $\delta^{13}C_{EC}$ values was not detected in other sympatric mammals from the Koobi Fora region, and local vegetation structures appear

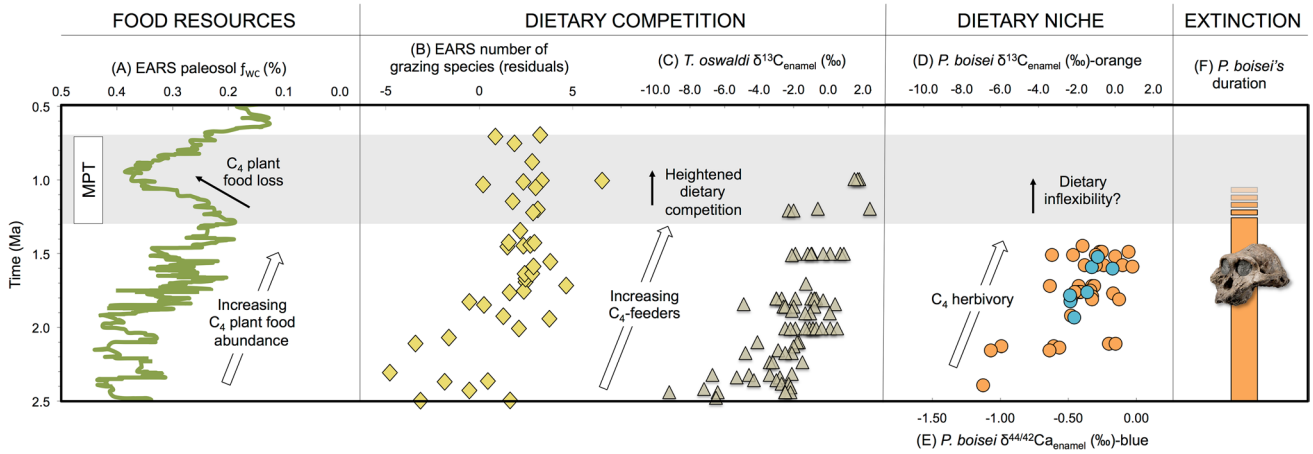

Figure 7. Proposed ecological and behavioral influences of *P. boisei's* extinction. Food resources represented by (**A**) EARS f_{WC} record (exponentially smoothed, $\alpha = 0.1$); dietary competition shown with (**B**) speciosity of EARS grazers[45] and (**C**) *T. oswaldi* $\delta^{13}C_{enamel}$ values; dietary niche shown with (**D**) *P. boisei* $\delta^{13}C_{enamel}$ and (**E**) $\delta^{44/42}Ca_{enamel}$ values; estimated time of extinction denoted by (**F**) *P. boisei's* duration[18]. See Supplementary Data and Supplementary Information for isotopic values, fossil image credit, and references. Shaded area denotes MPT interval (1.3–0.7 Ma).

stable; consequently, as these authors[63] suggest, it seems likely that a behavioral change rather than a change in resource base underpinned *H. erectus*' dietary shift. *H. erectus* and other members of *Homo* display wide ranges of $\delta^{44/42}Ca_{enamel}$ values after 1.65 Ma suggestive of omnivory (Fig. 1C). Ungulate C_4-grazer meat and marrow may have been the primary source of *H. erectus*' C_4 diet[13,63], supporting the interpretation of niche separation rather than direct competition between the hominin sister taxa even after 1.65 Ma. But notably a few *Homo* specimens approach *P. boisei's* $\delta^{13}C_{enamel}$ and $\delta^{44/42}Ca_{enamel}$ values[13], which could be interpreted to indicate that segments of the omnivorous *Homo* populations exploited some resources within *P. boisei's* dietary niche[12].

Similar biogeographic distributions and habitat preferences of members of *Homo* and *P. boisei*[62] implies competition for non-food resources including but not limited to feeding territories, sleeping sites, and potable water. Evidence for the origins[5,64] and evolution[65,66] of Early Stone Age technologies has shifted the discussion of presence vs. absence of tool making abilities by *P. boisei* and other non-*Homo* hominin species further toward the cognitive and social learning capacities required for habitual and advanced stone tool making[67]. The large-brained and -bodied *H. erectus* remains the most likely maker of advanced tools during the MPT interval[62] and may have outcompeted *P. boisei* for non-food resources and some C_4 plant foods with those tools.

In summary, EARS environments experienced a significant reduction in C_4 grasslands during the MPT interval potentially forced by an increase in pCO_2 and associated with a rise in temperature. The EARS C_3 excursion, peaking circa 1 Ma, escalated dietary competition amongst the abundant C_4-feeders, which influenced the decline of non-ruminant grazers. Dietary niche separation amongst the EARS hominins may have served as a strategy to reduce competition in the C_3-C_4-mixed feeding niche during the early Pleistocene. However, with C_4 plant food loss, *P. boisei's* inability to return to its ancestral C_3-C_4-mixed diet due to competitive exclusion by *H. erectus* and/or its own behavioral inflexibility likely played a role in its extinction (Fig. 7D–F).

Methods

Our study site is located in the Lake Turkana Basin, which is part of the northern Kenyan rift in the eastern branch of the EARS (Fig. 2A–C). On the northwest side of the basin, the Nariokotome Member is the uppermost unit of the Nachukui Formation and attains a thickness of ~ 60 m[69]. Previous interpretations suggested the Nariokotome Member was accumulated through the period of 1.30–0.75 Ma[70]. Near the Nariokotome Catholic mission, we studied this member's outcrops and sampled pedogenic nodules along two NW trending transects (Supplementary Fig. S1, Supplementary Table T1). Two representative composite stratigraphic sections, measuring 50–55 m thick, were recorded (Supplementary Fig. S6). Walking along marker horizons (e.g., stromatolites layers) or using a transit to level the relative positions of marker horizons facilitated correlations between successive outcrops (Supplementary Fig. S2). Sedimentary strata of these outcrops have dips of about 3–5° into the west or are nearly flat lying. The strata comprise rounded volcanic-clast gravels, quartzo-feldspathic sands of varying grain sizes, and mudstones. Locally, the mudstones preserve carbonate nodules and slickensided fractures that indicate paleosols. Occasionally interbedded with these detrital clastic sediments are thinner units of stromatolite-encrusted gravels, mollusk sandstones, and tuff layers.

On the northeast side of the basin, the Koobi Fora Formation's Chari Member (1.38–0.75 Ma) was examined because it is nearly time equivalent with the Nariokotome Member. We compiled fieldwork observations and samples from the Chari Member outcrops exposed near the town of Ileret (Supplementary Fig. S3). Sediments, chronostratigraphic constraints, and interpretations of the depositional environments for the Ileret outcrops have been described in detail elsewhere[39]. We sampled pedogenic carbonates from sedimentary strata documented by the section PNG-04[39] The PNG-04 section is redrawn in Supplementary Figure S4 and relevant latitude and

longitude data are listed in Supplementary Table T1. At PNG-04, an unconformity occurs ~ 7 m up from the base of the Chari Tuff. Samples were derived from stratigraphic levels above and below the unconformity, measured relative to the dated tuff units. Lithostratigraphic thicknesses, sedimentological data, and bedding attitudes were collected at the outcrops using standard field procedures and measuring instruments.

Pedogenic carbonate nodules were extracted from all preserved carbonate nodule-bearing paleosols throughout each of three outcrop sections in the Turkana Basin as the stratigraphic distribution of relevant geological materials dictated. Paleosols were identified from the presence of vertic features and slickensides. Pedogenic carbonate nodules were sampled at levels > 30 cm below the contact with overlying stratum and ~ 50 cm deep into the outcrop. Ages were determined through linear scaling between the stratigraphic levels of the radioisotopic dates of the Lower Nariokotome Tuff (1.30 Ma) and the Silbo Tuff (0.75 Ma) and the Chari Tuff (1.38 Ma) and the Silbo Tuff[70]. Scaled ages were calculated from the reported sedimentation rate[70]. The large age gap between samples Ileret 514–1 and 520–2 (Supplementary Fig. S5; Supplementary Data) is due to a ~ 500 kyr unconformity in the lower Chari Member (Supplementary Fig. S4)[39].

Pedogenic nodules were cross-sectioned to expose the inner surface. Carbonate powders were eroded with a hand-held rotary tool (Foredom Series) affixed with a 0.5 mm carbide bit. We avoided sparry calcite and collected micrite from the nodules. Ninety-five $\delta^{13}C$ analyses of extracted powders from fifty-three pedogenic carbonate (PC) nodules were conducted on a FISIONS Mass Spectrometer in the Department of Earth and Planetary Sciences at Rutgers University. Samples were reacted at 90 °C in 100% phosphoric acid for 13 min. $\delta^{13}C_{PC}$ and $\delta^{18}O_{PC}$ values are reported in the standard per mil (‰) notation: = $(R_{sample}/R_{standard} - 1)^*1000$, relative to Vienna-Pee Dee Belemnite (V-PDB) using the laboratory standard NBS-19. Analytical error is < 0.05‰.

We utilized $\delta^{13}C_{PC}$ data from published sources and this study (n = 53) to characterize vegetation structures in each of the EARS basins dated to 3–0 Ma, which spans the evolutionary history of *P. boisei* (Supplementary Data). Published data were taken from the compilation of Levin (2015)[23] and also from Quinn and others (2013)[71], Patterson and colleagues (2019)[63], and Potts et al. (2018)[72]. We then compiled $\delta^{13}C_{PC}$ values from EARS sampling locations that included data spanning the MPT interval to gauge relative changes in vegetation structures from 3 to 0 Ma, which included Awash, Turkana, Olduvai Gorge, and Tugen Hills. Due to potentially different rainfall sources across different EARS basins[73], we restricted time-series analysis to $\delta^{18}O_{PC}$ data from the Turkana Basin and Lower Omo Valley.

After Cerling and others[24] we subtracted 14‰ from the $\delta^{13}C_{PC}$ values to convert to the isotopic equivalent of organic carbon ($\delta^{13}C_{om}$) and used the equation: $f_{WC} = \{\sin[-1.06688 - 0.08538(\delta^{13}C_{om})]\}^2$ to generate estimates of fraction woody canopy cover (f_{WC}) for classification into UNESCO categories of African vegetation (see Supplementary Information). Eastern African savanna plant communities demonstrate a wide range of $\delta^{13}C_{PC}$ values, and due to differential paleosol deposition and preservation, $\delta^{13}C_{PC}$ data points are not evenly distributed through time. In order to assess trends in the central tendency of vegetation structures through time from the EARS f_{WC} datasets, we performed simple exponential smoothing (α = 0.1, 0.3, 0.6), Loess regressions (3%, 10%, 20%, 30%), and a Bayesian change point algorithm of a 5-point running mean (see Supplementary Information).

Received: 4 October 2020; Accepted: 18 March 2021
Published online: 30 March 2021

References

1. Leakey, L. S. B., Tobias, P. V. & Napier, J. R. A new species of the genus *Homo* from Olduvai Gorge. *Nature* **202**, 7–9 (1964).
2. Bromage, T. G. & Schrenk, F. Biogeographic and climatic basis for a narrative of early hominid evolution. *J. Hum. Evol.* **28**, 109–114 (1995).
3. Klein, R. The causes of "robust" australopithecine extinction in *Evolutionary history of the "robust" australopithecines* (ed. Grine, F.E.) 499–505 (Aldine de Gruyter, 1988).
4. McPherron, S.P. et al. Evidence for stone-tool-assisted consumption of animal tissues before 3.39 million years ago at Dikika, Ethiopia. *Nature* **466**, 857–860 (2010).
5. Harmand, S. et al. Before the Oldowan: 3.3 Ma Stone Tools from Lomekwi 3, West Turkana, Kenya. *Nature* **521**, 310–315 (2015).
6. Cerling, T. E. *et al.* Diet of *Panthropus boisei* in the early Pleistocene of East Africa. *Proc. Natl. Acad. Sci. USA* **108**, 9337–9341 (2011).
7. Ungar, P. S. & Sponheiner, M. The diets of early hominins. *Science* **334**, 190–193 (2011).
8. Cerling, T. E. *et al.* Stable isotope-based diet reconstructions of Turkana Basin hominins. *Proc. Natl. Acad. Sci. USA* **110**, 10501–10506 (2013).
9. Cerling, T. E. *et al.* Diet of *Theropithecus* from 4 to 1 Ma in Kenya. *Proc. Natl. Acad. Sci.* **110**, 10507–10512 (2013).
10. Ungar, P. S., Grine, F. E. & Teaford, M. F. Dental microwear and diet of the Plio-Pleistocene hominin *Paranthropus boisei*. *PLoS ONE* **3**, e2044 (2008).
11. Ludecke, T. *et al.* Dietary versatility of early Pleistocene hominins. *Proc. Natl. Acad. Sci. USA* **115**, 13330–13335 (2018).
12. Wynn, J. G. *et al.* Isotopic evidence for the timing of the dietary shift toward C_4 foods in eastern African *Paranthropus*. *Proc. Natl. Acad. Sci. USA* https://doi.org/10.1073/pnas.2006221117 (2020).
13. Martin, J. E., Tacail, T., Braga, J., Cerling, T. E. & Balter, V. Calcium isotopic ecology of Turkana Basin hominins. *Nat. Commun.* **11**, 3587 (2020).
14. Dominguez-Rodrigo, M. et al. First partial skeleton of a 1.34-million-year-old *Paranthropus boisei* from Bed II, Oluvai Gorge, Tanzania. *PLoS ONE* **8**, e80347 (2013).
15. Wood, B., Wood, C. & Konigsberg, L. *Paranthropus boisei*: An example of evolutionary stasis?. *Am. J. Phys. Anthropol.* **95**, 117–136 (1994).
16. Wood, B. A. & Patterson, B. A. *Paranthropus* through the looking glass. *Proc. Natl. Acad. Sci. USA* https://doi.org/10.1073/pnas.2016445117 (2020).
17. Antón, S. C., Potts, R. & Aiello, L. C. Evolution of early *Homo*: an integrated biological perspective. *Science* **345**, 1236828 (2014).
18. Wood, B. & Constantino, P. *Paranthropus boisei*: Fifty years of evidence and analysis. *Yrbk. Phys. Anthropol.* **50**, 106–132 (2007).
19. Muttoni, G., Scardia, G. & Kent, D. V. Early hominins in Europe: The Galerian migration hypothesis. *Quat. Sci. Rev.* **180**, 1–29 (2018).

20. Shultz, S., Nelson, E. & Dunbar, R. I. M. Hominin cognitive evolution: identifying patterns and processes in the fossil and archaeological record. *Phil. Trans. R. Soc. B* **367**, 2130–2140 (2012).
21. Clark, P. U. *et al.* The middle Pleistocene transition: characteristics, mechanisms, and implications for long-term changes in atmospheric *p*CO2. *Quat. Sci. Rev.* **25**, 3150–3184 (2006).
22. Raymo, M. E., Oppo, D. W. & Curry, W. The mid-Pleistocene climate transition: a deep sea carbon isotopic perspective. *Paleoceanogr.* **12**, 546–559 (1997).
23. Levin, N. E. Environment and climate of early human evolution. *Ann. Rev. Earth Planet. Sci.* **43**, 405–429 (2015).
24. Cerling, T. E. *et al.* Woody cover and hominin environments in the past 6 million years. *Nature* **476**, 51–56 (2011).
25. Potts, R. & Faith, J. T. Alternating high and low climate variability: the context of natural selection and speciation in Plio-Pleistocene hominin evolution. *J. Hum. Evol.* **87**, 5–20 (2015).
26. Cerling, T. E. *et al.* Dietary changes of large herbivores in the Turkana Basin, Kenya from 4 to 1 Ma. *Proc. Natl. Acad. Sci. USA* **112**, 11467–11472 (2015).
27. Negash, E. W. *et al.* Dietary trends in herbivores from the Shungura Formation, southwestern Ethiopia. *Proc. Natl. Acad. Sci. USA* https://doi.org/10.1073/pnas.2006982117 (2020).
28. Pasquette, J. & Drapeau, M. S. M. Environmental comparisons of the Awash Valley, Turkana Basin and lower Omo Valley from upper Miocene to Holocene as assessed from stable carbon and oxygen isotopes of mammalian enamel. *Palaeogeogr. Palaeoclimatol. Palaeoecol.* **562**, 110099 (2021).
29. Bobe, R. & Behrensmeyer, A. K. The expansion of grassland ecosystems in Africa in relation to mammalian evolution and the origins of the genus *Homo*. *Palaeogeogr. Palaeoclimatol. Palaeoecol.* **207**, 399–420 (2004).
30. Nutz, A. *et al.* Plio-Pleistocene sedimentation in West Turkana (Turkana Depression, Kenya, East African Rift System): paleolake fluctuations, paleolandscapes and controlling factors. *Earth-Sci. Rev.* **211**, 103415 (2020).
31. Sankaran, M. *et al.* Determinants of woody cover in African savannas. *Nature* **438**, 846–849 (2005).
32. Saji, N. H., Goswami, B. N., Vinayachandran, P. N. & Yamagata, T. A dipole in the tropical Indian Ocean. *Nature* **401**, 360–363 (1999).
33. Peterson, L. C., Haug, G. H., Hughen, K. A. & Rohl, U. Rapid changes in the hydrologic cycle of the tropical Atlantic during the Last Glacial. *Science* **290**, 1947–1951 (2000).
34. Schefuß, E., Schouten, S., Jansen, J.H.F., Sinninghe Damste, J.S. African vegetation controlled sea surface temperatures in the mid-Pleistocene period. *Nature* **422**, 418–421 (2003).
35. deMenocal, P.B. African climate change and faunal evolution during the Pliocene-Pleistocene. *Earth Planet. Sci. Lett.* **220**, 3–24 (2004).
36. Trauth, M. H., Maslin, M. A., Deino, A. & Strecker, M. R. Late Cenozoic moisture history of East Africa. *Science* **309**, 2051–2053 (2005).
37. Donges, J. F. *et al.* Nonlinear detection of paleoclimate-variability transitions possibly related to human evolution. *Proc. Natl. Acad. Sci. USA* **108**, 20422–20427 (2011).
38. Polissar, P. J., Rose, C., Uno, K. T., Phelps, S. R. & deMenocal, P. Synchronous rise of African C_4 ecosystems 10 million years ago in the absence of aridification. *Nat. Geosci.* **12**, 657–660 (2019).
39. Gathogo, P. N. & Brown, F. H. Stratigraphy of the Koobi Fora Formation (Pliocene and Pleistocene) in the Ileret region of northern Kenya. *J. Afr. Earth Sci.* **45**, 369–390 (2006).
40. Feibel, C. S. A geological history of the Turkana Basin. *Evol. Anthropol.* **20**, 206–216 (2011).
41. Faith, T. J., Rowan, J., Du, A. & Koch, P. L. Plio-Pleistocene decline of African megaherbivores: No evidence for ancient hominin impacts. *Science* **362**, 938–941 (2018).
42. Blumenthal, S. A. *et al.* Aridity and hominin environments. *Proc. Natl. Acad. Sci. USA* **114**, 7331–7336 (2017).
43. Lepre, C. J. Constraints on Fe-oxide formation in monsoonal Vertisols of Pliocene Kenya using rock magnetism and spectroscopy. *Geochem. Geophys. Geosyst.* **20**, 4998–5013 (2019).
44. Faurby, S., Silvestro, D., Werdelin, L. & Antonelli, A. Brain expansion in early hominins predicts carnivore extinctions in East Africa. *Ecol. Lett.* **23**, 537–544 (2020).
45. Faith, T. J., Rowan, J. & Du, A. Early hominins evolved within non-analog ecosystems. *Proc. Natl. Acad. Sci. USA* **116**, 21478–21483 (2019).
46. Bond, W. J., Midgley, G. F. & Woodward, F. I. The importance of low atmospheric CO_2 and fire in promoting the spread of grasslands and savannas. *Glob. Change Biol.* **9**, 973–982 (2003).
47. Bragg, F. J. *et al.* Stable isotope and modeling evidence for CO_2 as a driver of glacial-interglacial vegetation shifts in southern Africa. *Biogeosci.* **10**, 2001–2010 (2013).
48. Ehleringer, J. R., Cerling, T. E. & Helliker, B. R. C_4 photosynthesis, atmospheric CO_2, and climate. *Oecologia* **112**, 285–299 (1997).
49. Da, J., Zhang, Y., Li, G., Meng, X. & Ji, J. Low CO_2 levels of the entire Pleistocene epoch. *Nat. Commun.* **10**, 4342 (2019).
50. Stap, L. B. *et al.* CO_2 over the past 5 million years: continuous simulation and new $\delta^{11}B$-based proxy data. *Earth Planet. Sci. Lett.* **439**, 1–10 (2016).
51. van de Wal, R.S.W., de Boer, B., Lourens, LJ.., Kohler, P., Bintanja, R. Reconstruction of a continuous high-resolution CO_2 record over the past 20 million years. Clim. Past 7, 1459–69 (2011).
52. Passey, B. H., Levin, N. E., Cerling, T. E., Brown, F. H. & Eiler, J. M. High-temperature environments of human evolution in East Africa based on bond ordering in paleosol carbonates. *Proc. Nat. Acad. Sci. USA* **107**, 11245–11249 (2010).
53. Petit, J.R. et al. Climate and atmospheric history of the past 420,000 years from the Vostok ice core, Antarctica: *Nature* **399**, 429–436 (1999).
54. Schefuß, E. & Dupont, L. M. Multiple drivers of Miocene C4 ecosystem expansions. *Nat. Geosci.* **13**, 463–464 (2020).
55. Johnson, T.C. et al. A progressively wetter climate in southern East Africa over the past 1.3 million years. *Nature* **537**, 220–224 (2016).
56. Skonieczny, C. et al. Monsoon-driven Saharan dust variability over the past 240,000 years. *Sci. Adv.* **5**, eaav1887 (2019).
57. Caley, T. et al. A two-million-year-long hydroclimatic context for hominin evolution in southeastern Africa. Nature **560**, 76–79.
58. Kim, S.-J. *et al.* High-resolution climate simulation of the last glacial maximum. *Clim Dyn* **31**, 1–16 (2008).
59. Tierney, J. E., Russell, J. M., Sinninghe Damsté, J. S., Huang, Y. & Verschuren, D. Late quaternary behavior of the East African monsoon and the importance of the Congo Air Boundary. *Quatern. Sci. Rev.* **30**, 798–807 (2011).
60. Kingston, J. D. & Harrison, T. Isotopic dietary reconstructions of Pliocene herbivores at Laetoli: implications for early hominin paleoecology. *Palaeogeogr. Palaeoclimatol. Palaeoecol.* **243**, 272–306 (2007).
61. Quinn, R. L. Isotopic equifinality and rethinking the diet of *Australopithecus anamensis*. *Am. J. Phys. Anthropol.* **169**, 403–421 (2019).
62. Wood, D. Strait, Patterns of resource use in early Homo and Paranthropus. *J. Hum. Evol.* **46**, 119–162 (2004).
63. Patterson, D. B. *et al.* Comparative isotopic evidence from East Turkana supports a dietary shift within the genus *Homo*. *Nat. Ecol. Evol.* https://doi.org/10.1038/s41559-019-0916-0 (2019).
64. Lepre, C. J. *et al.* An earlier origin for the Acheulian. *Nature* **477**, 82–85 (2011).
65. Braun, D.R. et al. Earliest known Oldowan artifacts at >2.58 Ma from Ledi-Geraru, Ethiopia, highlight technological diversity. *Proc. Natl. Acad. Sci. USA* **116**, 11712–11717 (2019).

66. Mana, S., Hemming, S., Kent, D. V. & Lepre, C. J. Temporal and stratigraphic framework for paleoanthropology site within East-Central Area 130, Koobi Fora Kenya. *Front. Earth Sci.* **7**, 230 (2019).
67. Shea, J. J. Occasional, obligatory, and habitual stone tool use in hominin evolution. *Evol. Anthropol.* **26**, 200–217 (2017).
68. de la Torre, I. The origins of the Acheulean: past and present perspectives on a major transition in human evolution. *Philos. Trans. R. Soc. B* **371**, 20150245 (2016).
69. Harris, J. M., Brown, F. H. & Leakey, M. G. Geology and paleontology of Plio-Pleistocene localities west of Lake Turkana Kenya. *Contrib. Sci.* **399**, 1–128 (1988).
70. McDougall, I. *et al.* New single crystal $^{40}Ar/^{39}Ar$ ages improve time scale for deposition of the Omo Group, Omo-Turkana Basin East Africa. *J. Geol. Soc. Lond.* **169**, 213–226 (2012).
71. Quinn, R. L. *et al.* Pedogenic carbonate stable isotopic evidence for wooded habitat preference of early Pleistocene tool makers in the Turkana Basin. *J. Hum. Evol.* **65**, 65–78 (2013).
72. Potts, R. *et al.* Environmental dynamics during the onset of the Middle Stone Age in eastern Africa. *Science* **360**, 86–90 (2018).
73. Levin, N. E., Zipser, E. J. & Cerling, T. E. isotopic compositions of waters from Ethiopia and Kenya: insights into moisture sources for eastern Africa. *J. Geophys. Res.* **114**, D23306 (2009).

Acknowledgements

We thank the following for permissions, logistical support, and funding for field and laboratory work: Office of the President of Kenya, the Ministry of Education, Science and Technology, the National Council for Science and Technology, Kenya National Museums, Turkana Basin Institute, West Turkana Archaeological Project, The Leakey Foundation, US National Science Foundation (BCS-1455274; BCS-1818805), Richard Mortlock and James Wright at the Stable Isotope Laboratory in the Department of Earth and Planetary Sciences at Rutgers University. We posthumously thank Frank Brown for guidance during fieldwork at Nariokotome.

Author contributions

R.L.Q. and C.J.L. devised the study, conducted the data collection and analyses, interpreted the data, and wrote the paper.

Competing interests

The authors declare no competing interests.

Additional information

Supplementary Information The online version contains supplementary material available at https://doi.org/10.1038/s41598-021-86642-z.

Correspondence and requests for materials should be addressed to R.L.Q.

Reprints and permissions information is available at www.nature.com/reprints.

Publisher's note Springer Nature remains neutral with regard to jurisdictional claims in published maps and institutional affiliations.